BRAIN RESEARCH ▮ (▮▮▮▮) ▮▮▮–▮▮▮

Available online at www.sciencedirect.com

SciVerse ScienceDirect

www.elsevier.com/locate/brainres

Brain Research

Research Report

Brain-derived neurotrophic factor and the course of experimental cerebral malaria ☆

María Linares[a,b,1,2], Patricia Marín-García[a,b,1,3], Susana Pérez-Benavente[a], Jesús Sánchez-Nogueiro[c], Antonio Puyet[a,b], José M. Bautista[a,b,*], Amalia Diez[a,b]

[a]Department of Biochemistry and Molecular Biology IV, Universidad Complutense de Madrid, Ciudad Universitaria, 28040 Madrid, Spain
[b]Research Institute Hospital 12 de Octubre, Madrid, Spain
[c]Department of Toxicology and Pharmacology, Universidad Complutense de Madrid, Ciudad Universitaria, 28040 Madrid, Spain

ARTICLE INFO

Article history:
Accepted 21 October 2012

Keywords:
BDNF
Cerebral malaria
Adhesion molecule
Proteasome
Cytokine

ABSTRACT

The role of neurotrophic factors on the integrity of the central nervous system (CNS) during cerebral malaria (CM) infection remains obscure, but the long-standing neurocognitive sequelae often observed in rescued children can be attributed in part to the modulation of neuronal survival and synaptic plasticity. To discriminate the contribution of key responses in the time-sequence of the pathogenic events that trigger the development of neurocognitive malaria syndrome we defined four stages (I–IV) of the neurological progression of CM in C57BL/6 mice infected with *Plasmodium berghei* ANKA. Upregulation of ICAM-1, VCAM-1, e-selectin and p-selectin expression was detected in all cerebral regions before parasitized red blood cells (pRBC) accumulation. As the severity of symptoms increased, BDNF mRNA progressively diminished in several brain regions, earliest in the thalamus–hypothalamus, cerebellum, brainstem and cortex, and correlated with a four-stage disease sequence. Immunohistochemical confocal microscopy revealed changes in the BDNF distribution pattern, suggesting altered axonal transport. During CM progression, molecular markers of neurological infection and inflammation in the parasite and the host, respectively, were accompanied by a switch in the brain constitutive proteasome to the immunoproteasome, which could impede normal protein turnover. In parallel with BDNF downregulation, NCAM expression also diminished with increased CM severity. Together, these data suggest that changes in BDNF availability could be involved in the pathogenesis of CM.

Abbreviations: BDNF, brain-derived neurotrophic factor; CM, cerebral malaria; CNS, central nervous system; EC, endothelial cell; ECM, experimental cerebral malaria; GADPH, glyceraldehyde-3-phosphate dehydrogenase; ICAM-1, intercellular adhesion molecule; IFN-γ, interferon-γ; TNF-α, tumor necrosis factor-α; LT-α, lymphotoxin-α; NCAM, neural cell adhesion molecule; pRBC, parasitized red blood cells; VCAM-1, vascular cell adhesion molecule

☆ Presented in part: 7th European Congress on Tropical Medicine and International Health, Barcelona, Spain. October 2011 (abstract no. 147).

*Corresponding author at: Universidad Complutense de Madrid, Department of Biochemistry and Molecular Biology IV, Ciudad Universitaria, 28040 Madrid, Spain. Fax: +34 913943824.
E-mail address: jmbau@vet.ucm.es (J.M. Bautista).
[1] Both authors have contributed equally.
[2] Present address: Diseases of the Developing World, GlaxoSmithKline, 28760 Tres Cantos, Madrid, Spain.
[3] Present address: Department of Preventive Medicine, Public Health and Medical Immunology and Microbiology, Faculty of Health Sciences, Rey Juan Carlos University, Alcorcón, Madrid, Spain.

0006-8993/$ - see front matter © 2012 Elsevier B.V. All rights reserved.
http://dx.doi.org/10.1016/j.brainres.2012.10.040

1. Introduction

Cerebral malaria (CM) is the most important parasitic central nervous system (CNS) disease worldwide, accounting for 80% of all fatal cases of malaria. Although CM may be lethal in 15–30% of cases, it is potentially reversible (Armah et al., 2005; Bentivoglio et al., 2011). Most patients that survive CM make a full recovery, though long-standing neurocognitive sequelae are often observed, particularly in African children. Post-CM, impairments are observed in working memory, attention, language, hearing and vision and these may be accompanied by ataxia, hemiparesis or quadriparesis and epilepsy (Boivin et al., 2007; Idro et al., 2010a, 2010b). CM sequelae seem to be of multifactorial origin although their cause is largely unknown. A major role in triggering CM has been ascribed to microvascular obstruction by parasite adhesion and an exacerbated host inflammatory response (Lou et al., 2001). In a retrospective study, the severity of the clinical picture was linked to axonal injury (Medana et al., 2007) and neuronal damage has been identified to be a key process in CM (Anand and Babu, in press; Eeka et al., 2011). In this context, there is growing evidence that brain-derived neurotrophic factor (BDNF) is an important regulator of synaptogenesis and synaptic plasticity underlying learning and memory in the adult CNS. Moreover, BDNF promotes the survival and differentiation of neurons, axon regeneration and is involved in synaptic transmission (Cunha et al., 2010; Lu, 2003). Neuroprotection/neurotoxicity balance has been reported critical in CM development (Delahaye et al., 2007) and damaged synaptic transmission is also observed in CM (Marin-Garcia et al., 2009). All these suggest that BDNF could play a major role in the CM syndrome. Moreover, this central neurotrophin interacts with the proteasome system and neural cell adhesion molecule (NCAM), both attributed significant roles in neuronal survival and synaptic plasticity (Dong et al., 2008; Kiss et al., 2001; Seo et al., 2008). Hence, altered levels of any of these molecules give rise to CNS and behavioral impairments (Bingol and Sheng, 2011; Fukami et al., 2000; Rubinsztein, 2006). Pro-inflammatory cytokines produced during CM could induce immunoproteasome expression and proteasome switching to immunoproteasome (Groettrup et al., 2010; Nguyen et al., 2010). Host NCAM could also contribute to the sequestration of the parasitized red blood cells (pRBC) that provoke CM since it is capable of *in vitro* interacting with pRBC (Pouvelle et al., 2007). However, expression changes in NCAM produced during the course of CM have not yet been examined.

Given the role played by NCAM and BDNF in neurocognition (Bisaz et al., 2009; Zuccato and Cattaneo, 2009), these biomarkers were examined in parallel with the proteasome during the progression of experimental CM (ECM) in mice. Animals were clustered by neurological outcome to avoid the heterogeneity involved in the timing of disease events (Cabrales et al., 2010). In addition, the physiological functions of the different brain regions were independently considered,

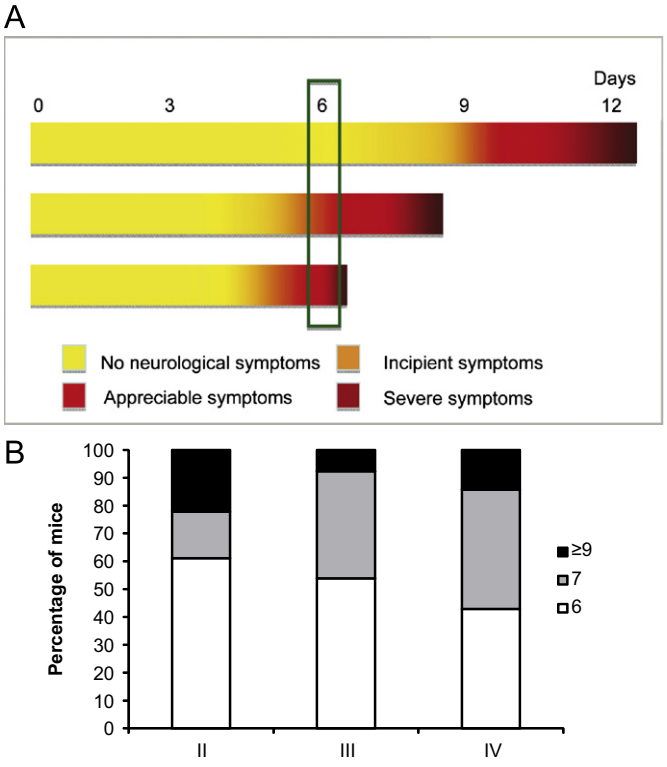

Fig. 1 – Clinical heterogeneity in progression of the neurological stages of ECM. (A) Clinical heterogeneity in CM progression observed in three representative mice (horizontal bars) within an experimental group. Vertical green bar illustrates heterogeneity at a given time point (day 6). (B) Percentage of mice that start developing CM stages (II, III or IV) at different times: day 6, day 7 or from day 9 to day 13 (≥9). (For interpretation of the references to color in this figure caption, the reader is referred to the web version of this article.)

Please cite this article as: Linares, M., et al., Brain-derived neurotrophic factor and the course of experimental cerebral malaria. Brain Research (2012), http://dx.doi.org/10.1016/j.brainres.2012.10.040

since specific damage in any region could lead to recognizable neurological symptoms and sequelae (Lackner et al., 2006; Marin-Garcia et al., 2009; Penet et al., 2005).

Here we demonstrate the reduced expression of brain-derived neurotrophic factor, constitutive proteasome and neural cell adhesion molecule in *Plasmodium berghei*-infected mouse brain dependent on the clinical severity of disease. Locally, inflammation markers as well as adhesion molecules precede the onset of parasite accumulation in the brain. Finally, in the four stages of cerebral malaria defined, neuroprotection markers in brain could be correlated with neurological signs.

2. Results

2.1. *Neurological course of CM in mice*

Since time-course studies during CM infection cannot be conducted in humans for obvious reasons, researchers have opted for the use of models of ECM such as infection of C57BL6/mice with *Plasmodium berghei* ANKA. Although these models might not reproduce all the features of human disease, they do recapitulate most of these features (de Souza et al., 2010; Hunt et al., 2006; Lou et al., 2001; Pierrot et al., 2003). In these models, disease severity is usually defined in terms of the number of days post infection (Delahaye et al., 2007; Lovegrove et al., 2007). However, in view of the heterogeneity observed in disease onset (Cabrales et al., 2010; de Souza et al., 2010), we classified the animals accordingly to neurological outcome.

In our study, infection levels and CM progression were assessed daily in individual mice by quantifying peripheral blood parasitemia and recording characteristic clinical symptoms of this syndrome. ECM mice showed progressive clinical changes, starting with early symptoms and later developing more specific neurological signs. Finally, animals lapsed into the most severe symptoms (Fig. 1 and Table 1). Stage I was defined as no neurological manifestations in the first few days of infection. Animals at this stage were neurologically indistinguishable from controls, although they presented parasitemia. Stage II was defined as the incipient symptoms of CM: head deviation or hemi-paralysis (Table 1). Some of these animals also exhibited ruffled fur, altered motility, weakness, tremor, rollover reaction and anemia (Table 1). From this stage, symptoms worsened rapidly. At stage III, neurological signs were appreciable: head deviation and or hemi-paralysis/paralysis, motionless, weakness and ruffled fur (Table 1). Finally, the most severe symptoms were observed in stage IV and included intense head deviation, severe hemi-paralysis/paralysis, motionless, intense weakness and ruffled fur (Table 1). Some animals assigned to stages III and IV also showed anemia, pelvic elevation, no response upon stimulation, tremor and swollen eyes (Table 1). Neurological outcome at each stage also considered the contingency response and spatial orientation displayed upon swimming.

It should be emphasized that, individually, ECM mice did not display the same symptoms at the same time (Fig. 1). Although initial symptoms were observed from day 6 as previously reported (Lou et al., 2001), temporal heterogeneity was observed in the appearance of stage II. Most severe stages (stages III and IV) were most often observed within 6–30 h after the first neurological symptoms appeared (stage II).

2.2. *BDNF expression pattern during the time-course of ECM*

bdnf mRNA levels were determined during the course of cerebral malaria in the main brain regions (olfactory bulb, hippocampus, frontal cortex, thalamus-hypothalamus, brainstem and cerebellum). *bdnf* was significantly and steadily downregulated until stage IV in all the cerebral regions examined (ranging from 4- to 7-fold depending on the cerebral region); the thalamus–hypothalamus, cerebellum, brainstem and cortex being the most affected areas (Table 2). This observed downregulation was inversely correlated with the increasing severity of neurological signs of infection. Based on these results, we then went on to examine BDNF expression also at the protein level. Care was taken to avoid antibody cross-reactivity between Plasmodium and the mouse housekeeping proteins used to normalize the data. Antibodies against mouse glyceraldehyde-3-phosphate dehydrogenase (GADPH), α-tubulin and β-actin were tested with a *P. berghei* protein extract and only anti-mouse GADPH showed no band of the expected size (Fig. 2A). Consequently this housekeeping protein was used for analysis of protein expression. BDNF protein expression levels were similar in control animals and those with stage IV CM (Fig. 2B). Next we compared the

Table 1 – Clinical symptoms associated with CM progression. Percentage of mice showing the different symptoms during the defined stages of disease from II to IV.

Stage	Ruffled fur	Motionless			Head deviation			Paralysis			Pelvic elevation	No response upon stimulation		Tremor	Weakness		Anemia	Eyes swollen	Roll-over
		I	A	S	I	A	S	I	A	S		Vis	Aud		A	S			
II	60	40	40	0	20	0	0	80	0	0	0	0	0	20	60	0	40	0	60
III	100	33	67	0	33[a]	67	0	0	83[b]	0	17	0	0	0	100	0	83	0	0
IV	100	0	29	71	0	57	43	0	0	100	29	43	29	29	14	86	57	14	0

I, incipient symptoms; **A**, appreciable symptoms; **S**, severe symptoms; **Vis**, visual; **Aud**, auditory.
[a] All animals which presented incipient signs of head deviation developed appreciable paralysis.
[b] All animals which not presented paralysis developed appreciable head deviation.

Please cite this article as: Linares, M., et al., Brain-derived neurotrophic factor and the course of experimental cerebral malaria. Brain Research (2012), http://dx.doi.org/10.1016/j.brainres.2012.10.040

immunohistochemical BDNF distribution pattern between control and CM mice at the most severe stage of the disease (stage IV). BDNF was detected in all analyzed regions. BDNF signal intensity was particularly high in cerebellum and preferently at the neuropil in granule layer in both control and CM mice (Fig. 3). In addition, a significantly higher ($P<0.05$) co-localization signal for BDNF and 4′-6-diamino-2-phenylindole (DAPI) was observed in infected mice (Pearson's correlation $=-0.13\pm0.03$) vs. control mice (Pearson's correlation $=-0.21\pm0.02$) whereas control animals showed a higher ($P<0.005$) co-localization signal for BDNF and α-tubulin (Pearson's correlation $=0.52\pm0.02$) vs. infected mice (Pearson's correlation $=0.41\pm0.02$).

2.3. *Proteasome and immunoproteasome subunit expression switching*

BDNF can interact with the proteasome system in such a way that proteasome inhibition blocks transcription of neurotrophins including *bdnf* (Dong et al., 2008). Further, diminished proteasome expression leads to the accumulation of misfolded proteins (Kwak et al., 2003), which may mask *bdnf* downregulation at the protein level. On the other hand, the inflammation produced during an infection is known to increase the expression of immunoproteasome subunits causing switching from the constitutive proteasome, which achieves normal protein processing through the ubiquitin system, to the immunoproteasome complex, which processes polypeptides for antigen presentation (Nguyen et al., 2010). This in turn leads to the accumulation of misfolded proteins. To investigate this switching from proteasome to immunoproteasome during CM progression, mRNA levels of the proteasome subunits *psmb*1 (β1) and *psmb*5 (β5) and their replacing immunoproteasome subunits *psmb*9 (*lmp*2) and *psmb*8 (*lmp*7) were analyzed. At the early asymptomatic stage I, immunoproteasome subunits *lmp*2 and *lmp*7 were found to be upregulated 5- to 10-fold in all brain areas, but more remarkably in the cerebellum (Table 3) and continuing into later CM stages. Conversely, the constitutive proteasome subunits β1 and β5 were gradually downregulated (approx. 2- to 4-fold, depending on the brain region) with the cerebellum and brainstem showing the most reduced levels (Table 3). This progressive downregulation of proteasome subunits β1 and β5 was correlated with increasing neurological signs in ECM mice and the mRNA expression of *bdnf* (Table S1).

Table 2 – Brain mRNA expression of *bdnf*. N-fold changes in the expression of *bdnf* mRNA in the brain regions in control mice (C) and mice at different CM stages (I–IV).

Region	Stage	Average	± SE
Cerebellum	C	−0.011	0.047
	I	−0.244	0.090
	II	−0.231	0.036
	III	−0.331	0.045
	IV	−0.604	0.097
Olfactory bulb	C	−0.008	0.040
	I	−0.096	0.042
	II	−0.132	0.066
	III	−0.427	0.066
	IV	−0.547	0.054
Brainstem	C	−0.010	0.047
	I	−0.253	0.055
	II	−0.225	0.045
	III	−0.465	0.083
	IV	−0.714	0.074
Frontal cortex	C	−0.018	0.064
	I	−0.209	0.065
	II	−0.425	0.022
	III	−0.653	0.062
	IV	−0.660	0.068
Hippocampus	C	−0.008	0.047
	I	−0.155	0.012
	II	−0.217	0.050
	III	−0.356	0.044
	IV	−0.331	0.075
Thalamus–hypothalamus	C	−0.118	0.163
	I	−0.493	0.076
	II	−0.725	0.024
	III	−0.613	0.175
	IV	−0.837	0.085

Data are the mean ± standard error (SE) of determinations made in 5–7 animals. *N*-fold change was calculated as the ratio between the amount of mRNA recorded for each mouse and the mean amount of mRNA detected in the control mice. *P* values for comparisons among the four groups in *bdnf* mRNA expression levels detected in the regions O.B., BS, CX, $P<0.001$ and CB, HIP, T–H, $P<0.005$.

2.4. *Early pro-inflammatory cytokine expression changes in the brain*

Overall, interferon-γ (IFN-γ), tumor necrosis factor-α (TNF-α) and lymphotoxin-α (LT-α) are pro-inflammatory cytokines known to participate in the pathogenesis of CM (Chen et al., 2000; Engwerda et al., 2002; Hunt and Grau, 2003; Lou et al., 2001; Weiser et al., 2007). However, it has also been established that IFN-γ and TNF-α cause the increased expression of immunoproteasome subunits (Groettrup et al., 2010). To examine a potential link between proteasome switching and local inflammation, mRNA expression of these three cytokines was determined in the different brain areas at clinical stage I, when the expression of the immunoproteasome subunits dramatically changes. At this asymptomatic stage, all brain areas exhibited almost identical cytokine mRNA expression patterns. Thus, with respect to the control mice, *ifn*-γ and *tnf*-α were significantly higher, between 10- and 200-fold, and *lt*-α showed identical expression levels (Fig. 4). The *ifn*-γ gene was the most upregulated, showing around 10-fold the expression shown by *tnf*-α in the cortex, hippocampus, thalamus–hypothalamus and brainstem.

2.5. *NCAM expression pattern and brain parasite load during ECM progression*

NCAM has been reported to interact with BDNF to mediate neuronal survival and plasticity (Kiss et al., 2001; Vutskits et al., 2001). The *in vitro* ability of this adhesion molecule to adhere pRBC (Pouvelle et al., 2007) suggests that it might also be involved in cytoadherence. Nevertheless, NCAM induction and its potential role in cytoadherence events or brain dysfunction during CM have not yet been elucidated. Cytoadherence is a specific CM outcome that consists of pRBC preferentially localized in the deep

Please cite this article as: Linares, M., et al., Brain-derived neurotrophic factor and the course of experimental cerebral malaria. Brain Research (2012), http://dx.doi.org/10.1016/j.brainres.2012.10.040

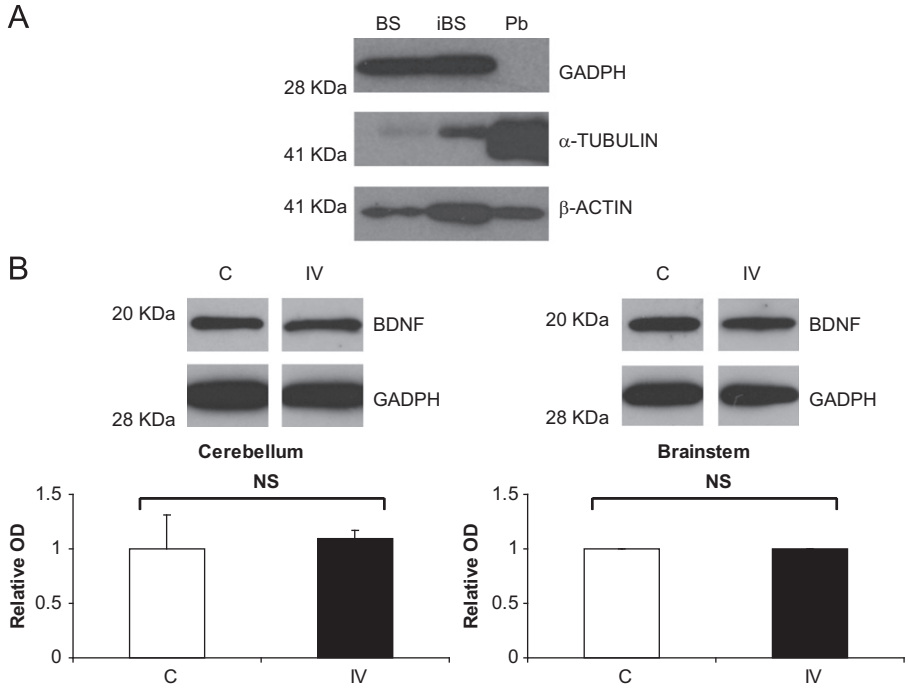

Fig. 2 – Protein expression of BDNF. *P. berghei* cross-reactivity of the antibodies against several murine housekeeping genes (A): Western blot showing GADPH, α-tubulin and β-actin immunoreactivity at the expected size of protein extracts from brainstem (BS), infected brainstem (iBS) and blood-isolated *P. berghei* (Pb). BDNF protein expression analysis (B): Western blot and densitometry used to determine BDNF and GADPH protein contents in the cerebellum and brainstem in control (C) and stage IV-CM (IV) mice. Relative optical density (OD) values given are the means ± standard errors recorded in four different animals, calculated as normalized expression of BDNF in each mouse relative to mean expression in control mice. NS, not significant.

vascular beds of body organs (mainly brain) preventing their removal by the spleen (Bentivoglio et al., 2011). The upregulation of other inducible adhesion molecules such as intercellular adhesion molecule (ICAM-1), vascular cell adhesion molecule (VCAM-1), p-selectin and e-selectin in CM brains (Armah et al., 2005; de Souza et al., 2010; Turner et al., 1994) suggests the interaction of several molecules as responsible for pRBC adhesion to blood vessels (Armah et al., 2005; Pino et al., 2005). However, there is no consensus on the sequence and timing of such cytoadherence events in CM (Combes et al., 2010; de Souza et al., 2010). Hence, to investigate NCAM in association with the other known cytoadherence players, mRNA expression levels of *ncam*, *icam*-1, *vcam*-1, *p-selectin* and *e-selectin* in parallel with parasite load were determined during the course of CNS infection.

In infected mice, each adhesion molecule exhibited a similar expression pattern in all the brain areas (Fig. 5). As expected, the expression of *e-selectin*, *p-selectin*, *icam*-1 and *vcam*-1 was significantly upregulated during CM progression. This event was observed early from asymptomatic stage I in all brain areas but most remarkably in cerebellum and brainstem (Fig. 5). The upregulation of these molecules continued into the remaining neurological stages (stages II–IV). The order of adhesion molecule expression upregulation levels was *e-selectin* > *icam*-1 > *p-selectin*~*vcam*-1, and the maximum increases observed from baseline levels were 40-, 10-, 4- and 3-fold respectively, depending on the brain region and disease stage.

Conversely, in the brain areas examined, *ncam* was significantly downregulated mainly in stages III and IV (from 2- to 3-fold, depending on the brain region), and again this downregulation was especially noticeable in the cerebellum and brainstem (Fig. 5).

The reported accumulation of pRBC in brain and peripheral tissues in the murine ECM model has raised some debate on their pathophysiological relevance (Amante et al., 2007; Baptista et al., 2010; Bentivoglio et al., 2011; Franke-Fayard et al., 2005). Hence, to compare pRBC accumulation during ECM between brain regions and peripheral tissues (including liver, lung and kidney), accurate parasite loads were determined by quantitative PCR. Peripheral blood samples obtained from ECM mice on the day of sacrifice at the different clinical stages (Fig. 6A) revealed low parasitemia levels during the course of infection. Although parasitemia increased significantly from controls to stage IV ($P<0.001$), the largest increase was produced from stages I to II (two-fold) and no significant differences were observed from stages II to IV, which is the time-period when the most severe symptoms develop. Parasite loads in peripheral tissues behaved similarly, including liver, lung and kidney (stages C-IV in lung, $P<0.005$; in liver and kidney, $P<0.001$). In these tissues, parasite loads failed to vary significantly once neurological symptoms appeared (Fig. 6B) unlike the behavior observed in the different brain regions (Fig. 6C). Thus, during the course of ECM, parasite loads increased in all brain regions (C-IV in all regions except thalamus–hypothalamus, $P<0.001$; thalamus–hypothalamus, $P<0.05$). In most brain areas, the build up of parasites was detected from stage II onwards, and increases were significant in the cerebellum ($P<0.05$), brainstem

Please cite this article as: Linares, M., et al., Brain-derived neurotrophic factor and the course of experimental cerebral malaria. Brain Research (2012), http://dx.doi.org/10.1016/j.brainres.2012.10.040

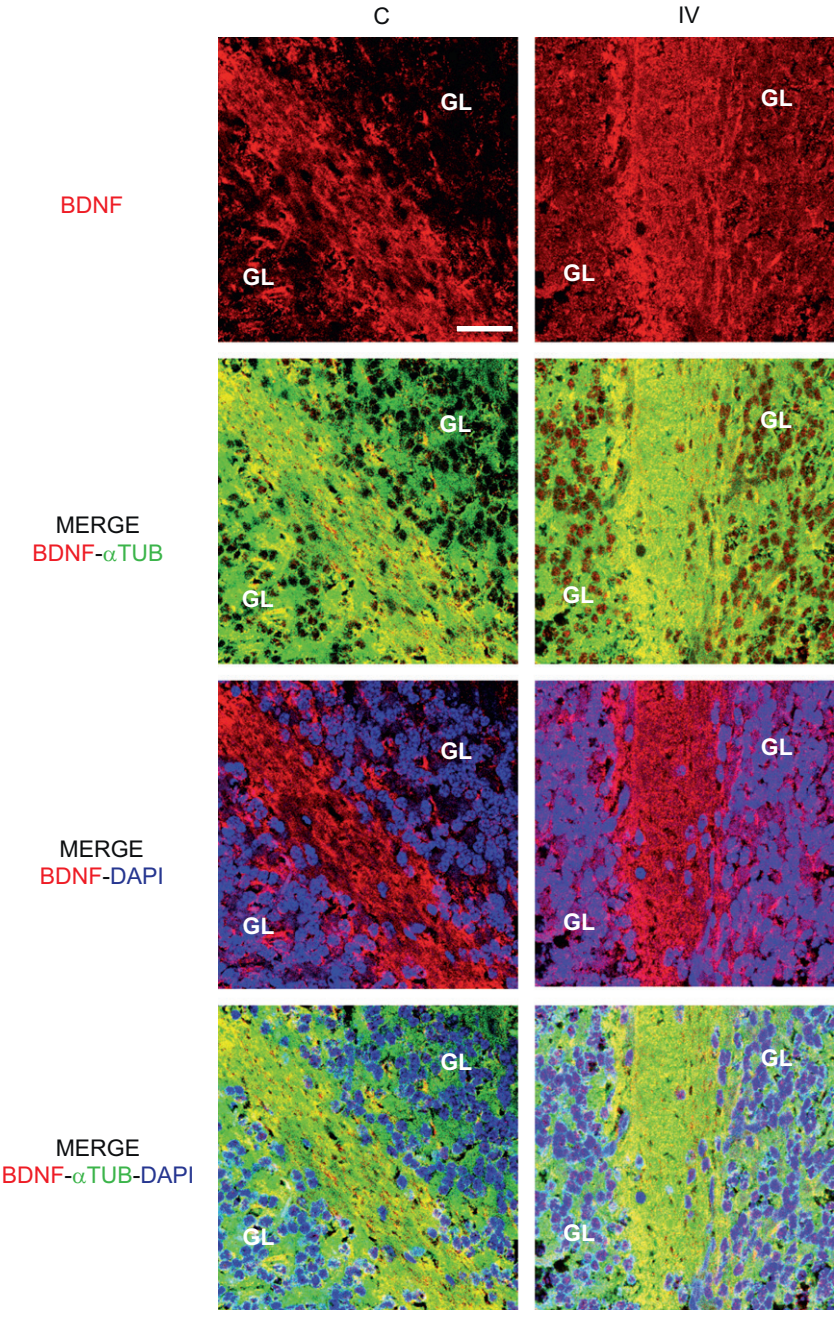

Fig. 3 – BDNF distribution in brain. Immunohistochemical distribution profiles of BDNF in brain slices obtained from the cerebellum in control (C) and CM mice at stage IV (IV). Images show the co-localization of BDNF (red), DAPI (blue) and α-tubulin (green). Granule layer, GL. Scale bar: 25 μm. (For interpretation of the references to color in this figure caption, the reader is referred to the web version of this article.)

($P<0.05$) and olfactory bulbs ($P<0.05$). Greatest accumulations of the parasite were observed at stage III (in the cerebellum, brainstem and thalamus–hypothalamus) or IV (in the olfactory bulbs and cortex) depending on the brain region. The highest numbers of pRBC per milligram of tissue were detected in the cerebellum (161.1 ± 31.9) and brainstem (196.2 ± 70.9) at stage III. The significant parasite accumulation observed from stage II and thereafter was positively correlated with the appearance of the most prominent neurological symptoms and therefore with the neurological outcome of infection and negatively correlated with the expression of *bdnf*, *ncam* and proteasome observed in most tissues (Table S2). Remarkably, when absolute amounts were compared, parasite loads (pBRC/mg) were up to 10-fold higher in peripheral tissue than brain (Fig. 6).

3. Discussion

Neurological sequelae are frequently observed in African children who survive CM (Idro et al., 2010a, 2010b). Since

Please cite this article as: Linares, M., et al., Brain-derived neurotrophic factor and the course of experimental cerebral malaria. Brain Research (2012), http://dx.doi.org/10.1016/j.brainres.2012.10.040

Table 3 – Brain mRNA expression of proteasome and immunoproteasome. N-fold changes in the expression of mRNA of the immunoproteasome subunits *lmp2* and *lmp7* and the proteasome subunits β1 (*prot* β1) and β5 (*prot* β5) in the brain regions in control mice (C) and mice at different disease stages (I–IV).

Region	Stage	*lmp2*		*lmp7*		*prot* β1		*prot* β5	
		Average	± SE	Average	± SE	Average	± SE	Average	± SE
Cerebellum	C	−0.007	0.039	−0.046	0.101	−0.002	0.019	−0.004	0.029
	I	1.005	0.048	1.104	0.059	−0.179	0.075	−0.217	0.054
	II	0.965	0.043	1.095	0.017	−0.237	0.018	−0.211	0.023
	III	1.109	0.039	1.274	0.047	−0.345	0.033	−0.386	0.048
	IV	1.328	0.208	1.248	0.054	−0.484	0.075	−0.611	0.090
Olfactory bulb	C	−0.023	0.070	−0.026	0.076	−0.001	0.017	−0.003	0.027
	I	0.744	0.121	0.742	0.168	−0.093	0.036	−0.099	0.051
	II	0.719	0.051	0.686	0.069	−0.173	0.033	−0.239	0.021
	III	0.744	0.032	0.742	0.036	−0.248	0.040	−0.386	0.066
	IV	0.729	0.036	0.780	0.029	−0.339	0.043	−0.438	0.038
Brainstem	C	−0.004	0.029	−0.011	0.048	−0.010	0.045	−0.006	0.036
	I	0.785	0.081	0.733	0.082	−0.123	0.047	−0.141	0.053
	II	0.922	0.024	0.841	0.057	−0.287	0.043	−0.289	0.039
	III	0.975	0.049	0.992	0.038	−0.393	0.042	−0.442	0.105
	IV	0.964	0.051	0.989	0.036	−0.537	0.029	−0.588	0.062
Frontal cortex	C	−0.009	0.044	−0.006	0.033	−0.003	0.026	−0.016	0.057
	I	0.849	0.081	0.846	0.082	−0.072	0.047	−0.152	0.066
	II	0.946	0.053	0.971	0.057	−0.130	0.006	−0.230	0.053
	III	1.043	0.032	1.064	0.039	−0.280	0.027	−0.329	0.042
	IV	0.968	0.048	1.007	0.050	−0.308	0.049	−0.360	0.063
Hippocampus	C	−0.017	0.062	−0.013	0.051	−0.003	0.027	−0.005	0.033
	I	0.883	0.066	0.794	0.078	−0.054	0.037	−0.096	0.049
	II	0.891	0.039	0.861	0.039	−0.098	0.024	−0.106	0.042
	III	1.013	0.039	1.007	0.055	−0.131	0.043	−0.197	0.055
	IV	0.952	0.045	0.993	0.051	−0.182	0.045	−0.277	0.031
Thalamus–hypothalamus	C	−0.014	0.052	−0.021	0.066	−0.027	0.076	−0.005	0.034
	I	0.812	0.069	0.764	0.054	0.060	0.070	−0.036	0.084
	II	0.902	0.044	0.896	0.021	−0.084	0.037	−0.182	0.061
	III	0.994	0.059	1.004	0.035	−0.223	0.042	−0.291	0.040
	IV	0.963	0.029	0.998	0.040	−0.273	0.031	−0.383	0.035

Data are the mean ± standard error (SE) of determinations made in 5–7 animals. The *N*-fold change for each subunit was calculated as the ratio between the amount of mRNA recorded for each mouse and the mean mRNA recorded in control mice. *P* values for comparisons among the four groups in mRNA expression levels of *prot* β1: CB, O.B., BS, CX, $P<0.001$; T–H, $P<0.005$; HIP, $P<0.05$; *prot* β5: CB, O.B., T–H, $P<0.001$; BS, CX, HIP, $P<0.005$; *lmp2*: CB, BS, CX, HIP, TAL, $P<0.005$; O.B., $P<0.01$; *lmp7*: BS, T–H, $P<0.001$; CB, O.B, CX, HIP, $P<0.005$.

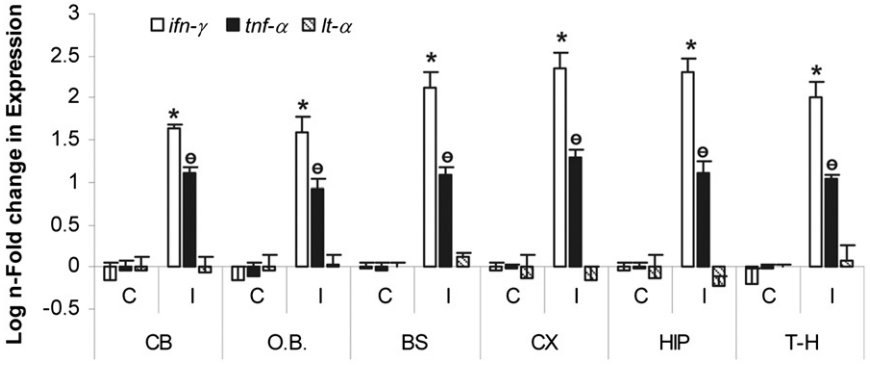

Fig. 4 – Brain mRNA expression of cytokines. mRNA expression levels of cytokines in the different brain regions. *N*-fold changes in mRNA expression levels of *ifn-γ*, *tnf-α* and *lt-α* detected in the cerebellum (CB), olfactory bulb (O.B.), brainstem (BS), frontal cortex (CX), hippocampus (HIP) and thalamus–hypothalamus (T–H) in control mice (C) and mice at CM stage I (I). Data are the means ± standard errors of determinations made in 3–6 animals. The *N*-fold change for each cytokine was calculated as the ratio between the amount of mRNA recorded for each mouse and the mean mRNA detected in control mice. Minor expression levels of *lt-α* were detected that did not vary between C and CM mice. ∗ indicates a significant difference in *ifn-γ* expression between control and CM stage I mice; [e] indicates a significant difference in *tnf-α* expression between control and CM stage I mice. ∗, [e]$P< 0.01$.

Please cite this article as: Linares, M., et al., Brain-derived neurotrophic factor and the course of experimental cerebral malaria. Brain Research (2012), http://dx.doi.org/10.1016/j.brainres.2012.10.040

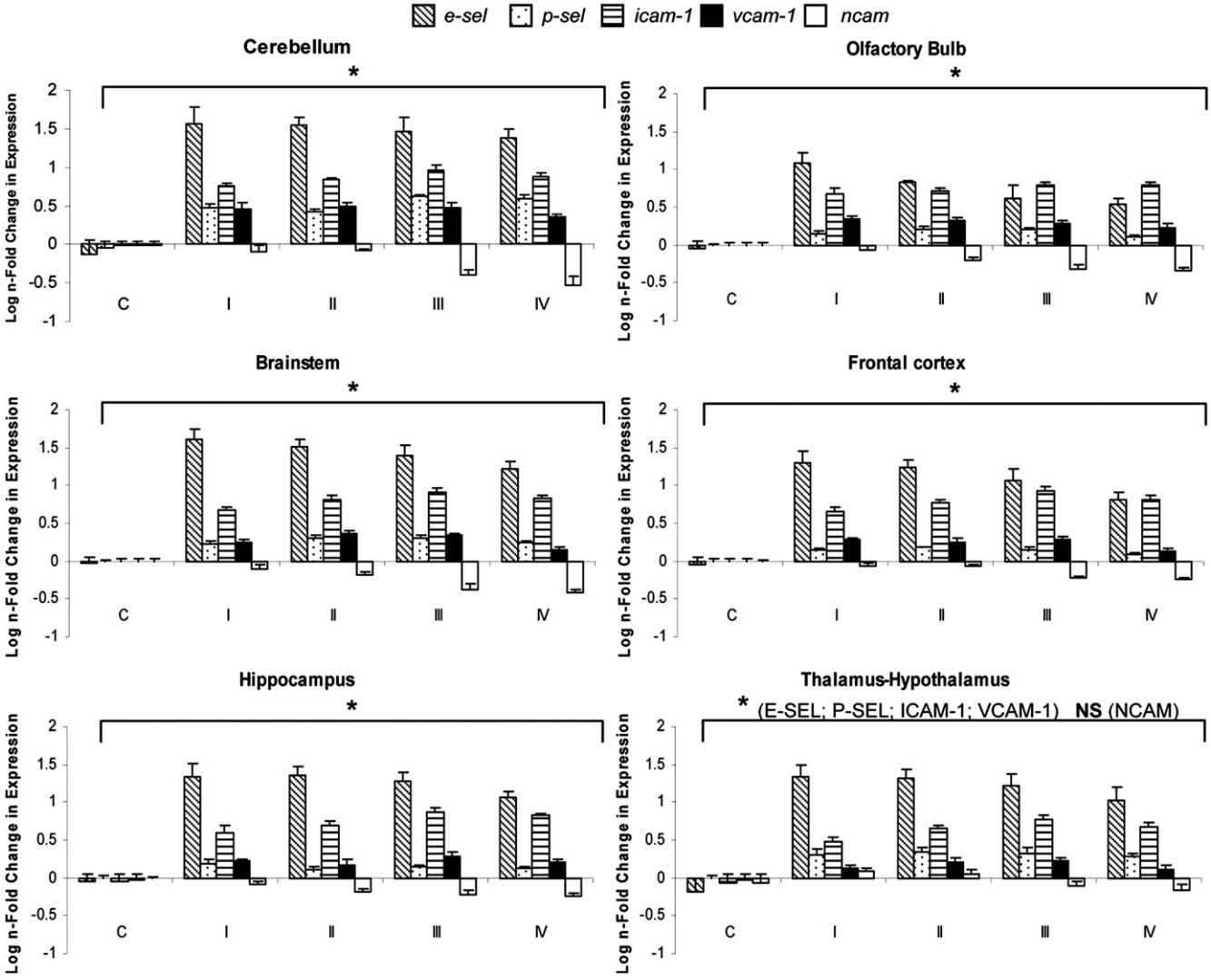

Fig. 5 – Brain mRNA expression of adhesion molecules. N-fold changes recorded in the expression of mRNA for *e-selectin* (*e-sel*), *p-selectin* (*p-sel*), *icam*-1, *vcam*-1 and *ncam* adhesion molecules in the cerebellum, olfactory bulb, brainstem, frontal cortex, hippocampus and thalamus–hypothalamus in control mice (C) and mice at the different CM stages (I–IV). Data are the means ± standard errors of determinations made in 5–7 animals. The N-fold change for each adhesion molecule was calculated as the ratio between the amount of mRNA recorded for each mouse and the mean mRNA detected in control mice. P values for comparisons among the four groups in adhesion molecule expression levels observed in the cerebellum: *icam*-1, *p-sel*, $P<0.001$; *vcam*-1, *ncam*, $P<0.005$; *e-sel*, $P<0.01$; olfactory bulb: *e-sel*, $P<0.001$; *icam*-1, *vcam*-1, *p-sel*, *ncam*, $P<0.005$; brainstem: *icam*-1, *vcam*-1, $P<0.001$; *e-sel*, *p-sel*, *ncam*, $P<0.005$; frontal cortex: *icam*-1, *ncam*, $P<0.001$; *vcam*-1, *e-sel*, $P<0.005$; *p-sel*, $P<0.01$; hippocampus: *icam*-1, $P<0.001$; *e-sel*, $P<0.005$; *ncam*, $P<0.01$; *vcam*-1, *p-sel*, $P<0.05$; thalamus–hypothalamus: *icam*-1, $P<0.001$; *e-sel*, $P<0.005$; *p-sel*, $P<0.01$; *vcam*-1, $P<0.05$. *$P<0.05$. NS, not significant.

BDNF is critical for neuronal survival, synaptic plasticity and cognitive processes (Greenberg et al., 2009), here we examined *bdnf* expression in ECM animals grouped together according to their neurological outcome. At the mRNA level, a gradual decrease in *bdnf* expression was observed that paralleled the progression of neurological symptoms (Linares et al., 2011b). *bdnf* downregulation could be responsible for altered pathways modulating cell survival, proliferation and differentiation in brain. *bdnf* expression is critical for neuron survival after injury (Ebadi et al., 1997). Thus, the changes observed in this marker might suggest the existence of a critical point of non-return for the neurocognitive deterioration observed in recovered patients. Detailed studies of CM in humans and mice have identified an array of neurological alterations including axonal injury and loss of endothelial cells and neurons (Eeka et al., 2011; Medana et al., 2007; Miu et al., 2008; Penet et al., 2005). Moreover, apoptosis markers have been shown to increase in the brain during CM progression (Anand and Babu, in press) in an inverse manner to the *bdnf* expression observed in this study. Since *bdnf* transcription relies upon neuronal activity (Lu, 2003), the loss of neurons in CM (Eeka et al., 2011) could also mediate the *bdnf* downregulation observed.

Please cite this article as: Linares, M., et al., Brain-derived neurotrophic factor and the course of experimental cerebral malaria. Brain Research (2012), http://dx.doi.org/10.1016/j.brainres.2012.10.040

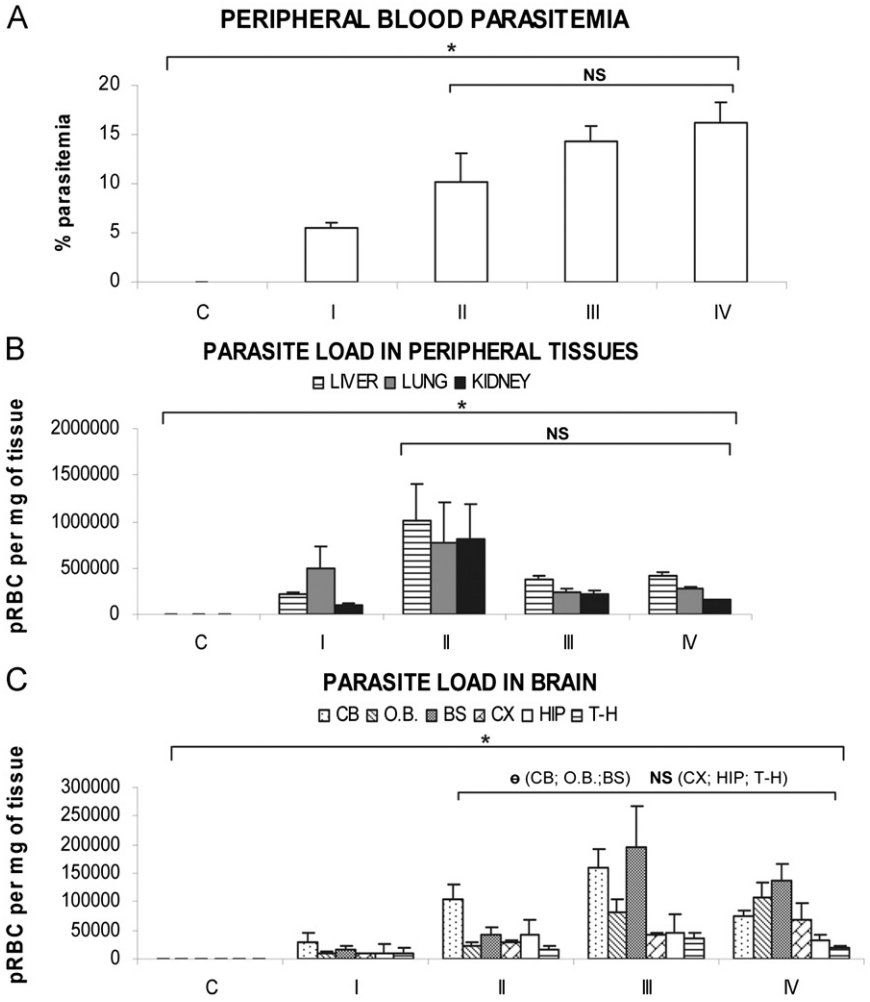

Fig. 6 – Parasite accumulation in brain, blood and peripheral tissues. Parasite loads detected in peripheral blood (A), peripheral tissue (B) and brain tissue (C) during CM progression. Brain areas analyzed: cerebellum (CB), olfactory bulb (O.B.), brainstem (BS), frontal cortex (CX), hippocampus (HIP) and thalamus–hypothalamus (T-H). Data are the means ± standard errors of determinations made in 4–6 animals. pRBC, infected red blood cells. C, control mice; I, disease stage I; II, stage II; III, stage III, IV, stage IV. * indicates a significant difference between groups C and IV; ^{e} indicates a significant difference between groups II and IV. *, $^{e}P<0.05$. NS, not significant.

Although changes in BDNF at the protein level were not observed, modified functionality of BDNF could account for the neurological deterioration that occurs during CM. Thus, mice at the most severe stage of the disease showed a preferential BDNF distribution in cell somas. Axonal transport modifications have been observed in human CM (Medana and Esiri, 2003), which could contribute to the altered BDNF distribution. The lack of diminished BDNF expression at the protein level can be explained by the observed downregulation of proteasome subunits β1 and β5, delaying protein turnover via the ubiquitin-proteasome pathway (Sommerfeld et al., 2000). In support of this hypothesis is the downregulation of other key molecules involved in the ubiquitin–proteasome pathway, such as the ubiquitin ligase complex, which mediates the polyubiquitination of misfolded proteins, recently reported in CM (Desruisseaux et al., 2010). In addition, hijacking of the constitutive proteasome by the immunoproteasome is a brain inflammatory response to viral infection that impedes normal protein turnover (Nguyen et al., 2010). TNF-α and IFN-γ are main inducers of proteasome immunosubunits (Groettrup et al., 2010) and thus, the early mRNA upregulation of these two pro-inflammatory cytokines, before any neurological symptoms appeared in our 4-stage model, suggests that inflammation could play a major role in the proteasome switching described here. The proteasome also participates in neuronal survival and plasticity (Dong et al., 2008; Gavilan et al., 2009; Kwak et al., 2003) and its dysfunction contributes to neurocognitive disturbances as a consequence of altered protein turnover impairing synaptic function (Bingol and Sheng, 2011; Nguyen et al., 2010). Thus, the association between BDNF transcriptional blockade and proteasome inhibition, reported also in other neurological malfunctions (Dong et al., 2008; Seo et al., 2008), could be responsible for the accelerated neurological deterioration that occurs during ECM in the mouse. Spatial memory training upregulates constitutive proteasome subunits and downregulates inducible ones (Gavilan et al., 2009) suggesting that the inflammatory

Please cite this article as: Linares, M., et al., Brain-derived neurotrophic factor and the course of experimental cerebral malaria. Brain Research (2012), http://dx.doi.org/10.1016/j.brainres.2012.10.040

induction of immunoproteasome in CM underlies, at least in part, cognitive impairment sequelae arising as a consequence of protein aggregation. This is consistent with the observation of detrimental effects of TNF-α and IFN-γ on brain protection and synaptic plasticity (Di Filippo et al., 2008).

In our 4-stage CM model, the expression of *ncam* was downregulated with increasing CM severity. NCAM plays a key role in neural development, cell migration, differentiation, survival, synaptogenesis, synaptic stabilization, and neuroplasticity (Bisaz et al., 2009). In addition, NCAM contributes to functional recovery and survival after injury (Kiss et al., 2001) and it is involved in learning and memory (Bisaz et al., 2009; Kiss et al., 2001; Vutskits et al., 2001). Moreover, NCAM interacts with BDNF to mediate neuronal survival and plasticity (Kiss et al., 2001; Vutskits et al., 2001). Interfering with NCAM function leads to cognitive impairment including deficits in learning, memory and emotions (Bisaz et al., 2009; Kiss et al., 2001).

In vitro studies have revealed that NCAM might participate in pRBC adhesion (Pouvelle et al., 2007). However, in our *in vivo* model, downregulation of *ncam* contrasts with the early upregulation of *icam*-1, *vcam*-1, *e-selectin* and *p-selectin* and the increasing brain parasitemia observed during the course of ECM, suggesting that NCAM is unlikely to play a role in pRBC adhesion to brain endothelium. In addition, these data suggest an early requirement of upregulated adhesion molecules for subsequent brain sequestration of pRBC, confirming previously reported findings (Armah et al., 2005; de Souza et al., 2010; Ho and White, 1999; Turner et al., 1994).

The pRBC sequestration in the brain of mice showing neurological signs of CM observed by us and other authors (Amante et al., 2007; Baptista et al., 2010; de Souza et al., 2010; Engwerda et al., 2002; Hearn et al., 2000; Lackner et al., 2006) contrasts with the findings of another study in which the build up of pRBC was only detected in peripheral tissue (Franke-Fayard et al., 2005). Whole body imaging and multi-organ comparisons could under-estimate pRBC accumulation since the signal from pRBC is likely to be much lower in the brain than in highly vascularized organs, where we also detected the largest parasite amounts but not their progressive increase.

According to our results, the inflammatory TNF-α and IFN-γ response could elicit pRBC accumulation by upregulating expression of *icam*-1, *vcam*-1, *e-selectin* and *p-selectin* (Armah et al., 2005; de Souza and Riley, 2002; Lou et al., 2001; Pino et al., 2005; Schofield and Grau, 2005; Turner et al., 1994; van der Heyde et al., 2006). Moreover, the early involvement of local cytokines could explain why cytokine-blocking antibody therapy is able to prevent but not reverse ECM (de Souza et al., 2010). Conversely, although a major role in *icam*-1 upregulation has been advocated for LT-α, this cytokine does not appear to mediate the early upregulation of adhesion molecules in our 4-stage neurological model. Hence, the reported high levels of LT-α in the last stage of ECM (Engwerda et al., 2002; Hunt et al., 2006) could be the consequence of later brain alterations.

In our study, major alterations were observed in cerebellum and brainstem, as previously reported (Lacerda-Queiroz et al., 2010; Lackner et al., 2006; Penet et al., 2005), which is in agreement with the neurological symptoms of CM including ataxia and impairment of movement and balance (Idro et al., 2005; Penet et al., 2005). The cerebellum is also one of the brain regions showing highest basal BDNF expression (Cunha et al., 2010). Further, greatest parasite accumulation during ECM was detected in the cerebellum, as reported elsewhere (Marin-Garcia et al., 2009; Sein et al., 1993). Since human CM brain sections (Armah et al., 2005) also show peak adhesion molecule expression in the cerebellum, this region seems to be the most damaged in both human and mouse CM.

In conclusion, the current study shows that the normalization of neurological scores in four stages during progression of cerebral malaria in mouse follows phenotypic changes in neuroinflammation markers and neuroplasticity mediators in parallel to pRBC sequestration (Fig. 7) thus, establishing a preclinical model for the evaluation of potential therapeutic agents to rescue cerebral malaria sequelae at the different phases of the disease. To this respect, since BDNF prevents cell death and reduces neurological signs of several CNS diseases (Zuccato and Cattaneo, 2009) and NCAM activates intracellular signaling cascades associated with cognitive processes (Bisaz et al., 2009) our findings suggest that these molecules could be a promising therapeutic target for modifying or reversing the neurocognitive effects of CM. Thus, although the direct implication of BDNF and its receptors in the protection mechanism remains to be investigated, glatiramer acetate, a compound that boosts BDNF expression (Aharoni et al., 2005), has been already shown to reduce the risk of developing ECM (Lackner et al., 2009). Similarly, new compounds modeled after binding sites of NCAM promote neuronal survival, modify cell adhesion and impair spatial learning (Kohler et al., 2010). Thus, these pharmacological tools and others are now amendable for *in vivo* analysis to restore expression levels of these new ECM biomarkers associated to neurocognitive phenotypes.

4. Experimental procedures

4.1. Ethics statement

All experiments with animals were conducted at the Universidad Complutense de Madrid in accordance with national and international regulations for animal experimentation and were performed with full adherence to the corresponding deontological and ethical guidelines. The study protocol was approved by the Committee of Animal Experimentation of the Universidad Complutense de Madrid on February 11 2010.

4.2. Animals and experimental infection

Five-week old male C57BL/6 mice were purchased from Harlan Ibérica (Barcelona, Spain). All animals were pathogen-free and were kept in our facilities at the Complutense University of Madrid, with free access to food and water. Twenty-four mice were intraperitoneally injected with 5×10^6 pRBC obtained from *P. berghei* (ANKA)-infected mice. Six uninfected mice served as controls. To minimize suffering and discomfort, the present study was conducted using non-injected control mice (Marin-Garcia et al., 2009). The choice of using non-injected animals was based on the national and international regulations regarding animal experimentation implemented at our University by the Committee of Animal

Please cite this article as: Linares, M., et al., Brain-derived neurotrophic factor and the course of experimental cerebral malaria. Brain Research (2012), http://dx.doi.org/10.1016/j.brainres.2012.10.040

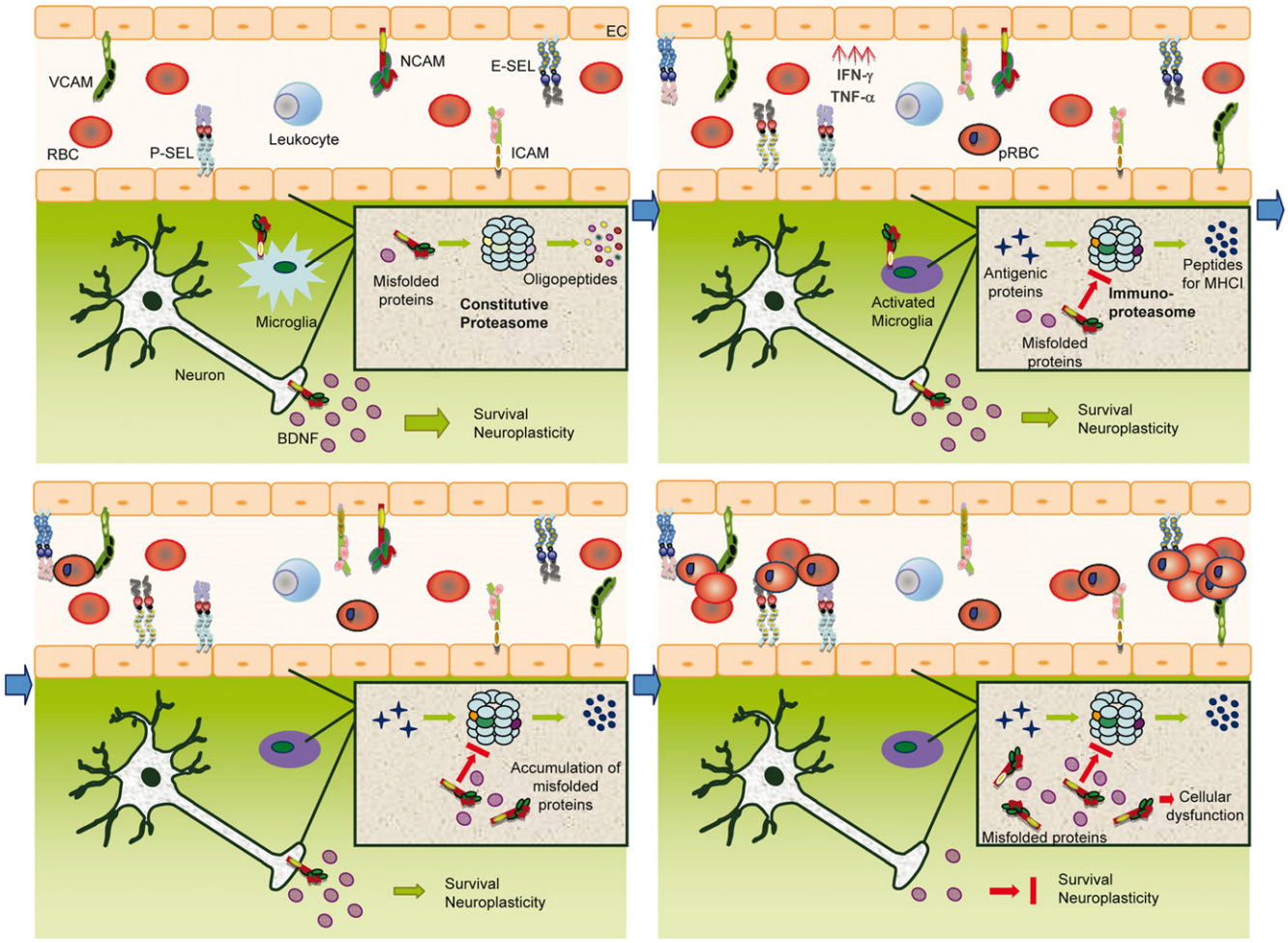

Fig. 7 – Physiopathological markers of ECM progression. The cartoon summarizes events hypothetically connected during the course of ECM. Thus, the early inflammatory cytokines TNF-α and IFN-γ could trigger pRBC accumulation by modulating the expression of ICAM-1, VCAM-1, *E*-selectin (E-SEL) and *P*-selectin (P-SEL). However, NCAM is unlikely to collaborate in pRBC adhesion to brain microvasculature. Reduced NCAM levels could be related to BDNF downregulation and proteasome dysfunction. Expression switching from the constitutive to immune subunits of the proteasome might promote the accumulation of misfolded proteins. Finally, BDNF, NCAM and proteasome downregulation could impair neural cell survival and neuroplasticity. EC: endothelial cell; RBC: red blood cell.

Experimentation aimed at minimizing animal suffering. According to preliminary experiments supported by previous reports (Marin-Garcia et al., 2009), injected and non-injected control mice showed identical behavior and histological phenotype during the experimental course, with no signs of disease or distress.

Infection progress was monitored daily by staining blood smears with Wright's eosin methylene blue solution (Merck) followed by pRBC counts under the microscope. Neurological symptoms in the animals were also monitored daily. The signs assessed were similar to the components of the SHIRPA score described previously (Amante et al., 2007; Lackner et al., 2006) and included ruffled fur, abnormal gait and reduced motility, tremor, reduced grip strength and weakness, affected auditory response, abnormal visual response, head deviation, hemi- or paraplegia, tendency to rollover on stimulation, pelvic elevation and swollen eyes. Infected animals were assigned to one of four disease stages (I–IV) depending on the severity of their neurological signs. At each stage, mice were sacrificed by cervical dislocation, decapitated and specimens obtained of peripheral tissue (lung, liver and kidney) and CNS tissue (olfactory bulb, frontal cortex, hippocampus, thalamus–hypothalamus, brainstem and cerebellum). To compare pRBC levels recorded in mice with human data, perfusion was not performed as recently suggested (de Souza et al., 2010).

4.3. *RNA expression analysis*

Total RNA was isolated from the olfactory bulb, hippocampus, frontal cortex, thalamus–hypothalamus, brainstem and cerebellum in control and CM mice using an ABI PRISM® 6100 Nucleic acid Prepstation following the manufacturer's instructions (Applied Biosystems). Reverse transcriptase reactions were performed using the High Capacity cDNA Archive Kit (Applied Biosystems). A 1:1 proportion of reverse transcriptase buffer to RNA was used.

Please cite this article as: Linares, M., et al., Brain-derived neurotrophic factor and the course of experimental cerebral malaria. Brain Research (2012), http://dx.doi.org/10.1016/j.brainres.2012.10.040

Cell adhesion molecule, BDNF and cytokine mRNA levels were determined by quantitative reverse transcriptase-PCR. Relative abundances of these molecules were determined using the 5′ fluorogenic nuclease assay (TaqMan) of the ABI 7700 Prism Sequence Detector system (Applied Biosystems). In separate PCR reactions, a commercial mixture was used of mouse specific primers and probes for *icam*-1, *vcam*-1, *ncam*, p-*selectin*, *e-selectin*, *bdnf*, *tnf*-α, *ifn*-γ, *lt*-α, immunoproteasome *lmp*2 and *lmp*7 subunits, proteasome β1 and β5 subunits and the housekeeping β-*actin* gene (TaqMan MGB probes). All PCR reactions were prepared with TaqMan PCR master Mix, No Amperase UNG (all from Applied Biosystems). The specificity of the primers and probes used was verified by basic local alignment search tool (BLAST) analysis comparing the mouse genes selected to the *Plasmodium berghei* genome and no significant similarity was found. The β-*actin* gene served as an endogenous control to check for slight variations in the initial concentration, total RNA quality and the conversion efficiency of the reverse transcription reaction. PCR reactions included an initial incubation of 10 min at 95 °C for polymerase activation, followed by 40 cycles (melting 15 s at 95 °C, annealing and extension 1 min at 60 °C) using an ABI PRISM 7000 Sequence Detection System (Applied Biosystems). Relative amounts of RNA were calculated by the comparative Ct method ($2^{-\Delta\Delta CT}$ method).

4.4. *Western blot analysis*

Total protein was extracted from the brainstem and cerebellum of control and CM mice as described previously (Linares et al., 2011a). Briefly, samples were homogenized in modified RIPA lysis buffer (50 mM Tris–HCl, pH8, 50 mM NaCl, 3% CHAPS and EDTA-free protease inhibitor cocktail), vortexed for 1 h at intervals of 10 min, centrifuged for 30 min and the extracted proteins recovered in the supernatants. About 25 μg of each protein extract were separated in a 10% SDS–acrylamide gel and transferred to nitrocellulose transfer membranes (Protran, Whatman). Membranes were blocked in a 5% milk phosphate buffer saline (PBS)-Tween 0.05% solution and probed with antibodies against BDNF (1/200, Santa Cruz Biotechnology) overnight at 4 °C. Membranes were then washed with PBS-Tween solution, incubated with horseradish peroxidase-conjugated anti-rabbit-IgG secondary antibody (1/2000, GE Healthcare), reacted in SuperSignal solution (Pierce) for 5 min, and exposed to a medical X-ray film (Agfa). Densitometry of blots was performed using Quantity-One 1-D analysis software (Bio-Rad). The housekeeping gene used to normalize the data was chosen after examining the specificity of several antibodies: GADPH, 1/4000, Applied Biosystems; α-tubulin, 1/10,000, Sigma-Aldrich; β-actin, 1/5000, Sigma-Aldrich) by comparing their reactivity with 9 μg of a mouse or *Plasmodium berghei* protein extract.

4.5. *Immunofluorescence assays*

Control and infected mice were sacrificed and whole brains removed and fixed overnight at 4 °C in 4% paraformaldehyde in PBS (w/v). After fixation, the brain tissue was subjected to a cryoprotective process. Sections of 10 μm were prepared using a Leica 3050 M cryostat. CM and control brain sections were incubated using the following primary antibodies: polyclonal rabbit anti-BDNF antibody at a 1:25 dilution from Santa Cruz Biotechnology and monoclonal mouse anti-α-tubulin at 1:500 from Sigma. Subsequently, the brain sections were washed with PBS buffer and incubated with secondary antibodies at the following dilutions: donkey anti-rabbit IgG labeled with indocarbocyanine, Cy3, (Jackson Immunoresearch Laboratories) (1:400) and goat anti-mouse IgG labeled with Alexa Fluor 488 from Invitrogen (1:400). Finally, the brain sections were washed in PBS, stained with DAPI, washed again in PBS and mounted following standard procedures. Blank slides were used to subtract any unspecific signal, following the same procedures but substituting the primary antibody with the same volume of PBS (Fig. S1). Both markers were analyzed by confocal microscopy taking successive Alexa Fluor and Cy3 fluorescence images using a Leica CTR 6500 fluorescence microscope (Leica Microsystems). Alexa Fluor was monitored by excitation with the 488-nm wavelength laser, Cy3 and DAPI were excited at wavelengths of 561 and 405 nm, respectively. The immunofluorescence images obtained were subjected to Pearson correlation analysis of co-localization of BDNF and α-tubulin or BDNF and DAPI using the automatic tool of the LAS-AF Lite software package from Leica Microsystems. A total of 13 images were analyzed in each group and correlation coefficients obtained in each experimental group were compared by Mann–Whitney tests.

4.6. *Quantifying tissue infection levels by quantitative PCR*

Tissue parasite loads are expressed as the number of pRBC per milligram of host tissue and determined by quantitative PCR as previously described (Marin-Garcia et al., 2009). Briefly, genomic DNA from the different peripheral tissue and brain regions was isolated using the TransPrep chemistry system of the ABI PRISM® 6100 Nucleic acid Prepstation, following the manufacturer's protocol (Applied Biosystems). Parasite and host DNA were subjected to quantitative PCR, amplifying the *P. berghei* (ANKA) *18S* and mouse β-*actin* genes in the same DNA sample in separate tubes using specific pairs of primers designed in our laboratory (Marin-Garcia et al., 2009) and the Fast SYBR Green Master Mix (Applied Biosystems). Amplification, data acquisition and data analysis were carried out using the ABI 7700 Prism Sequence Detector system. The amplification conditions were 20 s at 95 °C for enzyme activation and 40 cycles of 10 s at 95 °C and 30 s at 60 °C. Finally, the amount of host tissue and the number of pRBC present in each experimental sample were quantified by interpolating the corresponding CT values on two independent standard plots of a known log number of either parasites or milligrams of host tissue against amplification CT values, respectively (Fig. S2).

4.7. *Statistical analysis*

Data are presented as the mean ± standard error. Statistical analyses were performed using the SPSS 15.0 statistics package. The non-parametric tests U-Mann–Whitney and Kruskal–Wallis were used to compare two groups or more than two groups respectively. Correlations between two variables were assessed by Spearman correlation analysis. Statistical analyses were performed independently for each

Please cite this article as: Linares, M., et al., Brain-derived neurotrophic factor and the course of experimental cerebral malaria. Brain Research (2012), http://dx.doi.org/10.1016/j.brainres.2012.10.040

molecule and brain region. Differences between means were considered significant when the P value was <0.05.

Author's contributions

M.L. and P.M.G. designed and performed the experiments, collected, analyzed and interpreted the data, designed figures and tables and contribute to the writing; S.P.B. performed experiments; J.N.S. assisted with the confocal microscopy analyses; A.P. supervised experiments, interpreted data and revised manuscript; J.M.B. and A.D. supervised and designed the research, analyzed and interpreted the data and contribute to the writing.

Acknowledgments

We thank Dr. Ruth Gil-Prieto (URJ) and Dr. Stefan Walter (Harvard University) for statistical assistance, Ana Burton for reading and commenting on the manuscript. This work was supported by the Spanish Ministry of Innovation and Science (Grant BIO2010-17039) and by the Programme of Consolidated Research Teams from UCM-Comunidad de Madrid (Research Team 920267). M.L. did hold a FPU fellowship from the Spanish Ministry of Innovation and Science (AP20061576) at the time of performing the experimental work.

Appendix A. Supporting information

Supplementary data associated with this article can be found in the online version at http://dx.doi.org/10.1016/j.brainres.2012.10.040.

REFERENCES

Aharoni, R., Eilam, R., Domev, H., Labunskay, G., Sela, M., Arnon, R., 2005. The immunomodulator glatiramer acetate augments the expression of neurotrophic factors in brains of experimental autoimmune encephalomyelitis mice. Proc. Natl. Acad. Sci. U.S.A. 102, 19045–19050.

Amante, F.H., Stanley, A.C., Randall, L.M., Zhou, Y., Haque, A., McSweeney, K., Waters, A.P., Janse, C.J., Good, M.F., Hill, G.R., Engwerda, C.R., 2007. A role for natural regulatory T cells in the pathogenesis of experimental cerebral malaria. Am. J. Pathol. 171, 548–559.

Anand, S.S., Babu, P.P. Endoplasmic reticulum stress and neurodegeneration in experimental cerebral malaria. Neurosignals, http://dx.doi.org/10.1159/000336970, in press.

Armah, H., Wired, E.K., Dodoo, A.K., Adjei, A.A., Tettey, Y., Gyasi, R., 2005. Cytokines and adhesion molecules expression in the brain in human cerebral malaria. Int. J. Environ. Res. Public Health 2, 123–131.

Baptista, F.G., Pamplona, A., Pena, A.C., Mota, M.M., Pied, S., Vigario, A.M., 2010. Accumulation of Plasmodium berghei-infected red blood cells in the brain is crucial for the development of cerebral malaria in mice. Infect. Immun. 78, 4033–4039.

Bentivoglio, M., Mariotti, R., Bertini, G., 2011. Neuroinflammation and brain infections: historical context and current perspectives. Brain Res. Rev. 66, 152–173.

Bingol, B., Sheng, M., 2011. Deconstruction for reconstruction: the role of proteolysis in neural plasticity and disease. Neuron 69, 22–32.

Bisaz, R., Conboy, L., Sandi, C., 2009. Learning under stress: a role for the neural cell adhesion molecule NCAM. Neurobiol. Learn. Mem. 91, 333–342.

Boivin, M.J., Bangirana, P., Byarugaba, J., Opoka, R.O., Idro, R., Jurek, A.M., John, C.C., 2007. Cognitive impairment after cerebral malaria in children: a prospective study. Pediatrics 119, e360–e366.

Cabrales, P., Zanini, G.M., Meays, D., Frangos, J.A., Carvalho, L.J., 2010. Murine cerebral malaria is associated with a vasospasm-like microcirculatory dysfunction, and survival upon rescue treatment is markedly increased by nimodipine. Am. J. Pathol. 176, 1306–1315.

Combes, V., El-Assaad, F., Faille, D., Jambou, R., Hunt, N.H., Grau, G.E., 2010. Microvesiculation and cell interactions at the brain-endothelial interface in cerebral malaria pathogenesis. Prog. Neurobiol. 91, 140–151.

Cunha, C., Brambilla, R., Thomas, K.L., 2010. A simple role for BDNF in learning and memory?. Front Mol. Neurosci. 3, 1.

Chen, Q., Schlichtherle, M., Wahlgren, M., 2000. Molecular aspects of severe malaria. Clin. Microbiol. Rev. 13, 439–450.

de Souza, B.J., Hafalla, J.C., Riley, E.M., Couper, K.N., 2010. Cerebral malaria: why experimental murine models are required to understand the pathogenesis of disease. Parasitology 137, 755–772.

de Souza, J.B., Riley, E.M., 2002. Cerebral malaria: the contribution of studies in animal models to our understanding of immunopathogenesis. Microbes Infect. 4, 291–300.

Delahaye, N.F., Coltel, N., Puthier, D., Barbier, M., Benech, P., Joly, F., Iraqi, F.A., Grau, G.E., Nguyen, C., Rihet, P., 2007. Gene expression analysis reveals early changes in several molecular pathways in cerebral malaria-susceptible mice versus cerebral malaria-resistant mice. BMC Genom. 8, 452.

Desruisseaux, M.S., Iacobas, D.A., Iacobas, S., Mukherjee, S., Weiss, L.M., Tanowitz, H.B., Spray, D.C., 2010. Alterations in the brain transcriptome in *Plasmodium berghei* ANKA infected mice. J. Neuroparasitol. 1, 1–8.

Di Filippo, M., Sarchielli, P., Picconi, B., Calabresi, P., 2008. Neuroinflammation and synaptic plasticity: theoretical basis for a novel, immune-centred, therapeutic approach to neurological disorders. Trends Pharmacol. Sci. 29, 402–412.

Dong, C., Upadhya, S.C., Ding, L., Smith, T.K., Hegde, A.N., 2008. Proteasome inhibition enhances the induction and impairs the maintenance of late-phase long-term potentiation. Learn. Mem. 15, 335–347.

Ebadi, M., Bashir, R.M., Heidrick, M.L., Hamada, F.M., Refaey, H.E., Hamed, A., Helal, G., Baxi, M.D., Cerutis, D.R., Lassi, N.K., 1997. Neurotrophins and their receptors in nerve injury and repair. Neurochem. Int. 30, 347–374.

Eeka, P., Chaitanya, G.V., Babu, P.P., 2011. Proteolytic breakdown of cytoskeleton induces neurodegeneration during pathology of murine cerebral malaria. Brain Res. 1417, 103–114.

Engwerda, C.R., Mynott, T.L., Sawhney, S., De Souza, J.B., Bickle, Q.D., Kaye, P.M., 2002. Locally up-regulated lymphotoxin alpha, not systemic tumor necrosis factor alpha, is the principle mediator of murine cerebral malaria. J. Exp. Med. 195, 1371–1377.

Franke-Fayard, B., Janse, C.J., Cunha-Rodrigues, M., Ramesar, J., Buscher, P., Que, I., Lowik, C., Voshol, P.J., den Boer, M.A., van Duinen, S.G., Febbraio, M., Mota, M.M., Waters, A.P., 2005. Murine malaria parasite sequestration: CD36 is the major receptor, but cerebral pathology is unlinked to sequestration. Proc. Natl. Acad. Sci. U.S.A. 102, 11468–11473.

Fukami, E., Nakayama, A., Sasaki, J., Mimura, S., Mori, N., Watanabe, K., 2000. Underexpression of neural cell adhesion molecule and neurotrophic factors in rat brain following

thromboxane A(2)-induced intrauterine growth retardation. Early Hum. Dev. 58, 101–110.

Gavilan, M.P., Castano, A., Torres, M., Portavella, M., Caballero, C., Jimenez, S., Garcia-Martinez, A., Parrado, J., Vitorica, J., Ruano, D., 2009. Age-related increase in the immunoproteasome content in rat hippocampus: molecular and functional aspects. J. Neurochem. 108, 260–272.

Greenberg, M.E., Xu, B., Lu, B., Hempstead, B.L., 2009. New insights in the biology of BDNF synthesis and release: implications in CNS function. J. Neurosci. 29, 12764–12767.

Groettrup, M., Kirk, C.J., Basler, M., 2010. Proteasomes in immune cells: more than peptide producers?. Nat. Rev. Immunol. 10, 73–78.

Hearn, J., Rayment, N., Landon, D.N., Katz, D.R., de Souza, J.B., 2000. Immunopathology of cerebral malaria: morphological evidence of parasite sequestration in murine brain microvasculature. Infect. Immun. 68, 5364–5376.

Ho, M., White, N.J., 1999. Molecular mechanisms of cytoadherence in malaria. Am. J. Physiol. 276, C1231–C1242.

Hunt, N.H., Grau, G.E., 2003. Cytokines: accelerators and brakes in the pathogenesis of cerebral malaria. Trends Immunol. 24, 491–499.

Hunt, N.H., Golenser, J., Chan-Ling, T., Parekh, S., Rae, C., Potter, S., Medana, I.M., Miu, J., Ball, H.J., 2006. Immunopathogenesis of cerebral malaria. Int. J. Parasitol. 36, 569–582.

Idro, R., Jenkins, N.E., Newton, C.R., 2005. Pathogenesis, clinical features, and neurological outcome of cerebral malaria. Lancet Neurol. 4, 827–840.

Idro, R., Kakooza-Mwesige, A., Balyejjussa, S., Mirembe, G., Mugasha, C., Tugumisirize, J., Byarugaba, J., 2010a. Severe neurological sequelae and behaviour problems after cerebral malaria in Ugandan children. BMC Res. Notes 3, 104.

Idro, R., Marsh, K., John, C.C., Newton, C.R., 2010b. Cerebral malaria: mechanisms of brain injury and strategies for improved neurocognitive outcome. Pediatr. Res. 68, 267–274.

Kiss, J.Z., Troncoso, E., Djebbara, Z., Vutskits, L., Muller, D., 2001. The role of neural cell adhesion molecules in plasticity and repair. Brain Res. Rev. 36, 175–184.

Kohler, L.B., Christensen, C., Rossetti, C., Fantin, M., Sandi, C., Bock, E., Berezin, V., 2010. Dennexin peptides modeled after the homophilic binding sites of the neural cell adhesion molecule (NCAM) promote neuronal survival, modify cell adhesion and impair spatial learning. Eur. J. Cell. Biol. 89, 817–827.

Kwak, M.K., Wakabayashi, N., Greenlaw, J.L., Yamamoto, M., Kensler, T.W., 2003. Antioxidants enhance mammalian proteasome expression through the Keap1-Nrf2 signaling pathway. Mol. Cell. Biol. 23, 8786–8794.

Lacerda-Queiroz, N., Rodrigues, D.H., Vilela, M.C., Miranda, A.S., Amaral, D.C., Camargos, E.R., Carvalho, L.J., Howe, C.L., Teixeira, M.M., Teixeira, A.L., 2010. Inflammatory changes in the central nervous system are associated with behavioral impairment in *Plasmodium berghei* (strain ANKA)-infected mice. Exp. Parasitol. 125, 271–278.

Lackner, P., Beer, R., Heussler, V., Goebel, G., Rudzki, D., Helbok, R., Tannich, E., Schmutzhard, E., 2006. Behavioural and histopathological alterations in mice with cerebral malaria. Neuropathol. Appl. Neurobiol. 32, 177–188.

Lackner, P., Part, A., Burger, C., Dietmann, A., Broessner, G., Helbok, R., Reindl, M., Schmutzhard, E., Beer, R., 2009. Glatiramer acetate reduces the risk for experimental cerebral malaria: a pilot study. Malar. J. 8, 36.

Linares, M., Marin-Garcia, P., Mendez, D., Puyet, A., Diez, A., Bautista, J.M., 2011a. Proteomic approaches to identifying carbonylated proteins in brain tissue. J. Proteome Res. 10, 1719–1727.

Linares, M., Marin-Garcia, P., Perez-Benavente, S., Sanchez-Nogueiro, J., Puyet, A., Bautista, J.M., Diez, A., 2011b. Decreased levels of brain-derived neurotrophic factor across the neurological phenotype of cerebral malaria. Eur. J. Trop. Med. Int. Health 16 (S1), 147.

Lou, J., Lucas, R., Grau, G.E., 2001. Pathogenesis of cerebral malaria: recent experimental data and possible applications for humans. Clin. Microbiol. Rev. 14, 810–820.

Lovegrove, F.E., Gharib, S.A., Patel, S.N., Hawkes, C.A., Kain, K.C., Liles, W.C., 2007. Expression microarray analysis implicates apoptosis and interferon-responsive mechanisms in susceptibility to experimental cerebral malaria. Am. J. Pathol. 171, 1894–1903.

Lu, B., 2003. BDNF and activity-dependent synaptic modulation. Learn. Mem. 10, 86–98.

Marin-Garcia, P., Sanchez-Nogueiro, J., Diez, A., Leon-Otegui, M., Linares, M., Garcia-Palencia, P., Bautista, J.M., Miras-Portugal, M.T., 2009. Altered nucleotide receptor expression in a murine model of cerebral malaria. J. Infect. Dis. 200, 1279–1288.

Medana, I.M., Esiri, M.M., 2003. Axonal damage: a key predictor of outcome in human CNS diseases. Brain 126, 515–530.

Medana, I.M., Idro, R., Newton, C.R., 2007. Axonal and astrocyte injury markers in the cerebrospinal fluid of Kenyan children with severe malaria. J. Neurol. Sci. 258, 93–98.

Miu, J., Hunt, N.H., Ball, H.J., 2008. Predominance of interferon-related responses in the brain during murine malaria, as identified by microarray analysis. Infect. Immun. 76, 1812–1824.

Nguyen, T.P., Soukup, V.M., Gelman, B.B., 2010. Persistent hijacking of brain proteasomes in HIV-associated dementia. Am. J. Pathol. 176, 893–902.

Penet, M.F., Viola, A., Confort-Gouny, S., Le Fur, Y., Duhamel, G., Kober, F., Ibarrola, D., Izquierdo, M., Coltel, N., Gharib, B., Grau, G.E., Cozzone, P.J., 2005. Imaging experimental cerebral malaria in vivo: significant role of ischemic brain edema. J. Neurosci. 25, 7352–7358.

Pierrot, C., Adam, E., Lafitte, S., Godin, C., Dive, D., Capron, M., Khalife, J., 2003. Age-related susceptibility and resistance to Plasmodium berghei in mice and rats. Exp. Parasitol. 104, 81–85.

Pino, P., Taoufiq, Z., Nitcheu, J., Vouldoukis, I., Mazier, D., 2005. Blood–brain barrier breakdown during cerebral malaria: suicide or murder?. Thromb Haemost. 94, 336–340.

Pouvelle, B., Matarazzo, V., Jurzynski, C., Nemeth, J., Ramharter, M., Rougon, G., Gysin, J., 2007. Neural cell adhesion molecule, a new cytoadhesion receptor for *Plasmodium falciparum*-infected erythrocytes capable of aggregation. Infect. Immun. 75, 3516–3522.

Rubinsztein, D.C., 2006. The roles of intracellular protein-degradation pathways in neurodegeneration. Nature 443, 780–786.

Schofield, L., Grau, G.E., 2005. Immunological processes in malaria pathogenesis. Nat. Rev. Immunol. 5, 722–735.

Sein, K.K., Maeno, Y., Thuc, H.V., Anh, T.K., Aikawa, M., 1993. Differential sequestration of parasitized erythrocytes in the cerebrum and cerebellum in human cerebral malaria. Am. J. Trop. Med. Hyg. 48, 504–511.

Seo, H., Kim, W., Isacson, O., 2008. Compensatory changes in the ubiquitin-proteasome system, brain-derived neurotrophic factor and mitochondrial complex II/III in YAC72 and R6/2 transgenic mice partially model Huntington's disease patients. Hum. Mol. Genet. 17, 3144–3153.

Sommerfeld, M.T., Schweigreiter, R., Barde, Y.A., Hoppe, E., 2000. Down-regulation of the neurotrophin receptor TrkB following ligand binding. evidence for an involvement of the proteasome and differential regulation of TrkA and TrkB. J. Biol. Chem. 275, 8982–8990.

Turner, G.D., Morrison, H., Jones, M., Davis, T.M., Looareesuwan, S., Buley, I.D., Gatter, K.C., Newbold, C.I., Pukritayakamee, S., Nagachinta, B., et al., 1994. An immunohistochemical study of the pathology of fatal malaria. Evidence for widespread endothelial activation and a potential role for intercellular

Please cite this article as: Linares, M., et al., Brain-derived neurotrophic factor and the course of experimental cerebral malaria. Brain Research (2012), http://dx.doi.org/10.1016/j.brainres.2012.10.040

adhesion molecule-1 in cerebral sequestration. Am. J. Pathol. 145, 1057–1069.

van der Heyde, H.C., Nolan, J., Combes, V., Gramaglia, I., Grau, G.E., 2006. A unified hypothesis for the genesis of cerebral malaria: sequestration, inflammation and hemostasis leading to microcirculatory dysfunction. Trends Parasitol. 22, 503–508.

Vutskits, L., Djebbara-Hannas, Z., Zhang, H., Paccaud, J.P., Durbec, P., Rougon, G., Muller, D., Kiss, J.Z., 2001. PSA-NCAM modulates BDNF-dependent survival and differentiation of cortical neurons. Eur. J. Neurosci. 13, 1391–1402.

Weiser, S., Miu, J., Ball, H.J., Hunt, N.H., 2007. Interferon-gamma synergises with tumour necrosis factor and lymphotoxin-alpha to enhance the mRNA and protein expression of adhesion molecules in mouse brain endothelial cells. Cytokine 37, 84–91.

Zuccato, C., Cattaneo, E., 2009. Brain-derived neurotrophic factor in neurodegenerative diseases. Nat. Rev. Neurol. 5, 311–322.

Please cite this article as: Linares, M., et al., Brain-derived neurotrophic factor and the course of experimental cerebral malaria. Brain Research (2012), http://dx.doi.org/10.1016/j.brainres.2012.10.040